



## Distribution patterns and risks posed of polycyclic aromatic hydrocarbons contaminated in the surface sediment of the Red Sea coast (Egypt)

Ahmed El Nemr\*, Manal M. El-Sadaawy, Azza Khaled, Amany El-Sikaily

*Environmental Division, National Institute of Oceanography and Fisheries, Kayet Bay, El-Anfoushy, Alexandria, Egypt*

Tel. +201007801845; email: ahmedmoustafaelnemr@yahoo.com

Received 28 April 2013; Accepted 19 July 2013

---

### ABSTRACT

Coastal marine sediment samples collected from 17 locations along the Egyptian Red Sea coast in June 2009 were analyzed for aliphatic, polycyclic aromatic hydrocarbons (PAHs), and total organic carbon (TOC). Total concentrations of 16 Polycyclic Aromatic Hydrocarbons-Environmental Protection Agency (EPA-PAHs) in the studied sediment samples varied from 0.132 to 5.182  $\mu\text{g g}^{-1}$  with an average value of 1.628  $\mu\text{g g}^{-1}$  (dry weight). The total aliphatic concentrations fluctuated between 4.232 and 71.874  $\mu\text{g g}^{-1}$  with an average value of 23.022  $\mu\text{g g}^{-1}$  (dry weight). The carcinogenic PAHs (PAH<sub>CARC</sub>) concentrations were ranged between 0.063 and 3.522  $\mu\text{g g}^{-1}$  (dry weight). The highest PAHs contents found in the samples from Ras Suder (5.182  $\mu\text{g g}^{-1}$ ), El-Tour (4.052  $\mu\text{g g}^{-1}$ ), and Sharm (3.367  $\mu\text{g g}^{-1}$ ) locations. Good correlations were observed between the individual PAHs concentrations. The average total organic carbon percent (TOC%) varied between not-detected and 0.35%. The concentration of total pyrolytic hydrocarbons ( $\Sigma\text{COMB}$ ) was higher than the total fossil hydrocarbons ( $\Sigma\text{PHE}$ ), which indicated that the atmospheric fall-out was the significant source of PAHs to the Red Sea marine sediments. Principal component analysis (PCA) was used to determine the sources of hydrocarbon pollutants in the Red Sea sediments. Additionally, individual PAHs compound ratios suggested the pyrogenic origins. Human hazard risk assessment of PAHs was also studied to evaluate the possible risk of contaminated sediments to the public health concerning PAHs intakes.

*Keywords:* Surface sediment; PAHs; Red Sea; Pollution monitoring; Hydrocarbons; Health risk assessment; PCA

---

### 1. Introduction

Polycyclic aromatic hydrocarbons (PAHs) are a group of ubiquitous environmental pollutants, some of which are known to be mutagenic or carcinogenic

[1–3]. The United States Environmental Protection Agency has listed 16 PAHs as priority pollutants in wastewater and 24 PAHs in soils, sediments, hazardous solid waste, and groundwater [4,5]. PAHs have been utilized extensively for source assessments [6–9]. Fossil fuel combustion, waste incineration, coal gasification and liquefaction processes, petroleum refining,

---

\*Corresponding author.

production of coke, carbon black, coal tar, pitch and asphalt, and biomass burning have been identified as important anthropogenic sources of PAHs [10]. PAHs have been released into marine environments via industrial wastewater, sewage, road runoff/street dust, and as petroleum through oil spills and ship traffic [5,11]. Aliphatic hydrocarbons can be of both petrogenic and biogenic origin, while PAHs can be petrogenic, pyrolytic, and biogenic. They arise from the incomplete combustion of organic material, especially fossil fuels (pyrolytic origin), from the discharge of petroleum and its products (petrogenic origin) and from the postdepositional transformation of biogenic precursors (diagenetic origin). Terrestrial plant waxes, marine phytoplankton, volcanic eruptions, biomass combustion, and natural oil seeps contribute as natural inputs of aliphatic and aromatic hydrocarbons [12–14].

The aliphatic hydrocarbons comprise *n*-alkanes, branched alkanes, isoprenoids, and cyclic compounds, including geochemical biomarkers, such as hopanes and steranes. Both aliphatic hydrocarbons and PAHs are often used to identify hydrocarbon sources. Their analysis can be used to fingerprint spilled oils. They also provide additional information on the source of hydrocarbon contamination and the extent of degradation of the oil spill [14]. Because of their low aqueous solubilities and high octanol–water partition coefficient ( $\log K_{ow}=3.4\text{--}7.6$ ), PAH compounds in aquatic system tend to be associated with sediments and biota with reported cases of toxicity, carcinogenicity, and mutagenicity [15].

Sediments are recognized as excellent sinks for pollutants, such as the hydrocarbons of interest. These compounds are readily adsorbed on particulate material. Bottom sediments act as a reservoir for hydrophobic contaminants. Therefore, sediments can hold and release pollutants, causing detrimental effects to biota long after the input of pollution has ceased [16].

The effect of PAHs is usually widespread and permanent in environmental media, and thus, PAHs can be eventually deposited and persistent in bed sediments (as a sink) in the aquatic system. This occurs because most PAHs, with their high hydrophobicity, sorb strongly to the organic in sediments and are resistant to bacterial degradation in an anoxic environment. Under favorable environmental conditions, PAHs may be released to the water as a continuing source and threaten the aquatic marine ecosystem through bioaccumulation in food chains [17]. Levels of PAHs in sediments vary, depending on the proximity of the sites to areas of human activity [18]. The analysis of sediment PAHs can serve as a

useful index of the contamination level and the source of PAHs input to the aquatic environments [19]. To characterize PAHs distribution better, the molecular indices based on the ratios of various selected PAHs have been widely used to characterize their origins [20–22]. These ratios are based on the differences in the physicochemical behavior of various structural isomers. For example, phenanthrene/anthracene and fluoranthene/pyrene are two pairs of isomers whose difference in reactivity and solubility proves useful in providing a tracer of PAHs from its origin [22,23]. In this study, gas chromatography (GC) and gas chromatography mass techniques were used to identify the types and to assess the sources of representative PAHs in the samples collected from 17 locations along the Egyptian Red Sea coast. In context, the importance of this research is to study the risk assessment of sediments contaminated by PAHs.

## 2. Materials and methods

### 2.1. Collection and preparation of sediment samples

Surface sediment samples were collected from seventeen different locations along the Egyptian Red Sea coast during June 2009 (Fig. 1). The locations were selected according to the expected polluted areas that are affected by the industrial and human activities (Table 1). Sediments were collected utilizing a stainless-steel grab. Six grabs were taken from each location from which the top 5 cm was scooped into precleaned wide-mouth glass bottles, frozen, transported to the laboratory and stored at  $-20^{\circ}\text{C}$  until analysis. The boat was moved up to 4–6 m between grabs so that the samples would be representatives of the area from which they were taken. The samples were prepared for aliphatic and aromatic hydrocarbons following well-established techniques [24,25]. The samples were analyzed for aliphatic and aromatic hydrocarbons, grain size distribution, total organic carbon (TOC%), and total organic matter (TOM%). About 3–4 g of each sample was oven-dried at  $105^{\circ}\text{C}$  to a constant weight to obtain percentage water content.

### 2.2. Grain size analysis

Grain size analysis was carried out using the conventional method [26,27]. Raw samples were treated with 30% (v/v) hydrogen peroxide solution to destroy the organic matter content, and about 100 g of the sediment was dried at  $105^{\circ}\text{C}$  and subsequently placed in the topmost sieve, and the entire column of

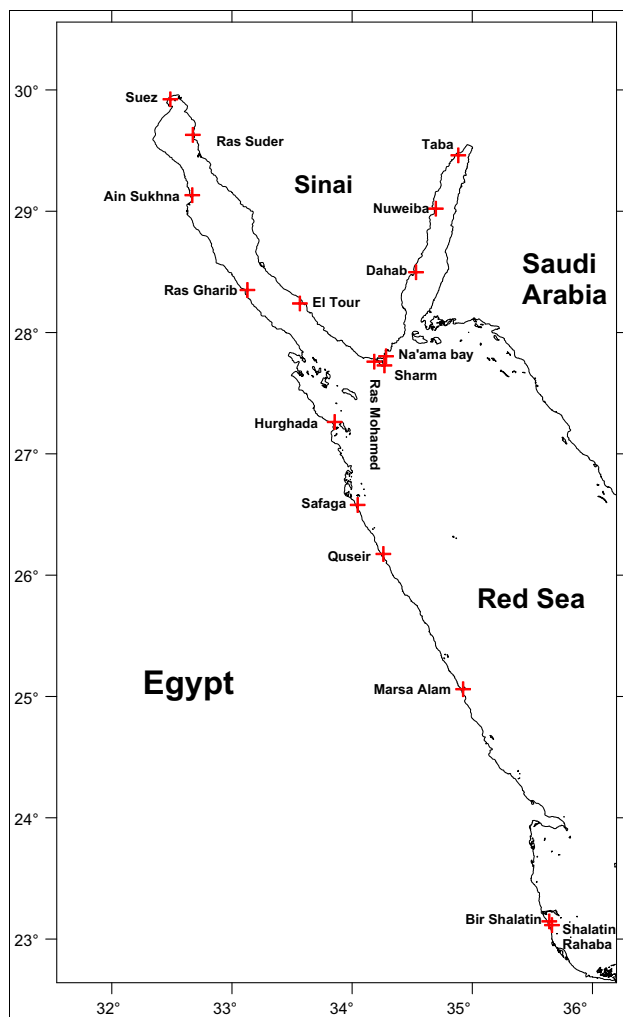


Fig. 1. Sampling locations along the Egyptian Red Sea coast.

Table 1  
Sources of pollution and other impacts and the main sites of pollution in the Red Sea

Sources of pollution and other impacts	Main sites of pollution
Offshore oil platforms (oil discharge originating from production water, oil-contaminated cutting, well testing, spill due to negligence or malpractice accidents)	Ain Sukhan (oil terminate for SUMED oil pipeline)
Ships (oil loading and unloading, discharge of oil ballast, tank washing and bilge oil)	El Tour and Ras Gharib
Shipment of mineral products (mainly phosphor)	Safaga and Quseir

sieves was subsequently deposited on sediments. The sieve meshes give the glass intervals 2, 1, 0, 0.5, 0.2, 0.125, and 0.063 mm. The data for grain size analysis were reported in (Table 2).

### 2.3. Extraction of hydrocarbons

Individual samples were removed from the refrigerator and allowed to thaw at room temperature for 5 h. Each sample was then thoroughly mixed, and 30 g of the sediment was mixed with 90 g of anhydrous sodium sulfate. Duplicates were taken from each sediment sample. The sediment samples were sonicated in an ultrasonic bath with 2 × 100 ml hexane for 30 min each, followed by a third extraction with 100 ml dichloromethane. The three extracts were combined and desulfurized through activated copper powder and then concentrated to a few milliliters in a rotary evaporator at low temperature (~35°C), followed by concentration with nitrogen gas stream down to a volume of 2 ml. Clean-up and fractionation was performed by passing the concentrated extract through a silica/aluminum oxide column.

The chromatography column was prepared by slurry packing 20 ml (10 g) of silica, followed by 10 ml (10 g) of aluminum oxide and finally 1 g of anhydrous sodium sulfate. The extract (2 ml) was sequentially eluted from the column with 25 ml of hexane for the saturated aliphatic fraction (F1) followed by 60 ml of hexane/dichloromethane (80:20) for the unsaturated and aromatic hydrocarbons fraction (F2). F1 and F2 were concentrated to 1.5 ml using a gentle stream of nitrogen for instrumental analysis.

### 2.4. Analytical quality controls

To control the analytical reliability and assure recovery efficiency and accuracy of the results, 6 analyses were conducted on the PAH compounds reference materials IAEA-408, as well as the sediment samples of known PAH levels which were spiked with a mixture consisting of 2 µg each of PAHs and were analyzed as above to validate the analytical method used in this study. The lowest detection limit (LDL) was 0.02 µg ml<sup>-1</sup> for lower molecular mass compounds, while indeno [1,2,3-cd] pyrene has LDL of 0.1 µg ml<sup>-1</sup>. The recovery efficiency ranged from 96.3 to 105.2% for IAEA-408 (Table 3) and 95 to 105.1% for the spiked samples. The mean recovery for PAHs were as follows: Naph 95.5%, Achy 93.8%, Ace 104.5%, F1 103.7%, Phe 97.3%, Ant 105.1%, Flu 92.8%, Pyr 90.8%, BaA 90.3%, Chr 106.4%, BaP 96.2%, BbF 88.6%, DBA 99.8%, BghiP 92.6%, and InP 94.9%.

Table 2  
 Characterization of the coastal surface sediments of the Red Sea during 2009

Location	St. no.	Position (°)	WC%	CO <sub>3</sub> %	TOC%	TOM%	Sand%	Silt%	Mud%	Sorting	Sediment type
Taba	1	34.88°E; 29.46°N	15.03	2	0.35	0.62	94.83	5.10	0.00	0.79	Medium Sand
Nuweiba	2	34.69°E; 29.02°N	8.33	6	0.20	0.36	99.51	0.14	0.05	1.40	Coarse sand
Dahab	3	34.53°E; 28.50°N	8.09	22	0.25	0.45	99.26	0.71	0.04	1.27	Coarse sand
Na'ama Bay	4	34.28°E; 27.80°N	21.01	14	0.01	0.018	97.77	2.19	0.04	1.29	Coarse sand
Ras Mohamed	5	34.19°E; 27.76°N	8.71	10	0.01	0.002	93.33	6.67	0.00	1.77	Medium Sand
Sharm	6	34.27°E; 27.72°N	26.8	18	0.198	0.356	93.10	6.90	0.00	1.69	Coarse sand
El Tour	7	33.56°E; 28.24°N	31.8	22	0.198	0.356	96.01	3.05	0.94	0.82	Medium Sand
Ras Suder	8	32.67°E; 29.13°N	19.45	56	0.30	0.53	98.15	1.61	0.25	0.61	Medium Sand
Suez	9	32.67°E; 29.63°N	21.19	2	0.247	0.446	99.95	0.03	0.03	1.25	Coarse sand
Ain Sukhna	10	32.49°E; 29.92°N	17.48	54	0.10	0.20	95.70	4.30	0.00	0.63	Fine sand
Ras Gharib	11	33.13°E; 28.35°N	23.26	28	1.75	3.15	99.78	0.22	0.00	0.00	Coarse sand
Hurghada	12	33.85°E; 27.26°N	24.04	24	0.04	0.09	99.72	0.20	0.08	0.54	Medium Sand
Safaga	13	34.06°E; 26.58°N	24.91	6	0.17	0.31	97.66	2.34	0.00	0.61	Medium Sand
Quseir	14	34.26°E; 26.17°N	19.33	2	0.15	0.27	84.34	15.66	0.00	1.35	Fine sand
Marsa Alam	15	34.92°E; 25.06°N	20.28	2	0.30	0.54	99.66	0.24	0.10	1.30	Coarse sand
Shalatin-1	16	35.66°E; 23.12°N	22.23	43	0.346	0.62	98.32	1.64	0.04	0.64	Fine sand
Shalatin-2	17	35.64°E; 23.15°N	20.67	44	0.346	0.62	99.15	0.82	0.00	0.77	Fine sand

Table 3  
Reference material IAEA-408 (PAHs concentration found in  $\text{ng g}^{-1}$ ) and total *n*-alkanes ( $\text{C}_{14} - \text{C}_{34}$   $\mu\text{g g}^{-1}$ )

Hydrocarbons	Requested	Found	Recovery%
Naphthalene	27	26.6	98.6
Anthracene	9.8	9.4	96.3
Fluoranthene	84	86.6	103.1
Pyrene	77	74.5	96.7
Benzo[a]anthracene	53	54.1	102.1
Chrysene	35	34.8	99.3
Benzo[b]fluoranthene	46	47.9	104.2
Benzo[a]pyrene	48	50.5	105.3
Benzo[ghi]perylene	38	37.7	99.1
Total <i>n</i> -alkane ( $\text{C}_{14} - \text{C}_{34}$ )	8.1	8.3	102.1

Concentrations reported in this study were not corrected for recovery rates.

## 2.5. Chemical

Silica gel and aluminum oxide used for column chromatography were solvent extracted with *n*-hexane in a glass cartridge inserted into an extraction apparatus, as described by Ehrhardt [28]. After extraction, they were first dried in the same cartridge with a nitrogen stream, activated by heating the cartridge in an electric tube oven to 200°C for 6 h, and then partially deactivated with 5% water and stored in amber bottle. All solvents were pesticides grade purchased from BDH. Anhydrous sodium sulfate was extracted with *n*-hexane in a Soxhlet apparatus for 8 h and then with methanol or dichloromethane for another 8 h, precombusted in a muffle furnace at approximately 400°C overnight and cooled in a greaseless desiccators.

## 2.6. GC analyses

Blanks of 1,000-fold concentration (1,000 ml of the solvent used was concentrated to 1 ml) were analyzed by Gas Shimadzu Class LC-10 equipped with Shimadzu Auto-injector, split/splitless injector and a fused silica capillary B-5 (30 m, 0.32 mm, 0.17  $\mu\text{m}$ ) 100% dimethylpolysiloxane and a FID detector. The temperature was programmed from 60 to 300°C with a rate of 5°C  $\text{min}^{-1}$  and was then maintained at 290°C for 25 min. The injector and detector temperatures were set at 280 and 300°C, respectively. Helium was used as the carrier (1.5 ml  $\text{min}^{-1}$ ) and nitrogen as the makeup (60 ml  $\text{min}^{-1}$ ) gas. Concentrations of individually resolved peaks were summed to obtain the total PCB concentration. Two microliters volume of each sample was injected in the split mode (1:10), and the

purge time was 1 min. The response factor of individual PAH compounds to the internal standard was measured and calculated at least three times at the beginning, in the middle, and at the end for each batch of GC injections (8 samples). Identification and quantification of 16 PAH compounds were based on matching their retention time with a mixture of PAH standards. Compound identification was confirmed by GC coupled to mass spectrometry in the chemical ionization mode and negative ion recording (Trace DSQ II Ms with capillary column: Thermo TR-35 MS Mass Selective Detector. Ion repeller was 1.5 V). Data were scanned from  $m/z$  50 to 450 at 1 s per decade. Data were also acquired in selected ion-monitoring mode with a dwell time and span of 0.06 s and 0.10 a.m.u., respectively. The 16 PAH compounds were naphthalene (Naph,  $m/z$  128), acenaphthalene (Acth,  $m/z$  152), acenaphthene (Ace,  $m/z$  154), fluorene (Fl,  $m/z$  166), phenanthrene (Phe,  $m/z$  178), anthracene (Ant,  $m/z$  178), fluoranthene (Flu,  $m/z$  202), pyrene (Pyr,  $m/z$  202), benzo[a]anthracene (BaA,  $m/z$  228), chrysene (Chr,  $m/z$  228), benzo[b]fluoranthene (BbF,  $m/z$  252), benzo[k]fluoranthene (BkF,  $m/z$  252), benzo[a]pyrene (BaP,  $m/z$  252), benzo[ghi]perylene (BghiP,  $m/z$  278), indeno[1,2,3-cd]pyrene (InP,  $m/z$  278), and dibenzo[a,h]anthracene (DBA,  $m/z$  278).

## 2.7. Total carbonate, TOC%, and TOM%

The TOC content was determined by oxidation with 1 N ( $\text{K}_2\text{Cr}_2\text{O}_7$ ) followed by acidification with concentrated  $\text{H}_2\text{SO}_4$  and then titrated against 0.5 N  $[\text{Fe}(\text{NH}_4)_2(\text{SO}_4)_2]$  [29]. Total carbonate was estimated as described by Molnia [30].

## 2.8. Risk assessment

### 2.8.1. Incidental ingestion of sediment

2.8.1.1. *Exposure data.* Incidental ingestion of sediment may occur during recreational activities such as swimming or wading. The intake equation includes different intake scenarios for children and adults to account for the likelihood that children will ingest more sediments than adults.

2.8.1.2. *Estimated dose.* (i) Chronic daily intake of incidental ingestion of sediments is estimated as follows in Eq. (1) [31]:

$$\text{Intake (mg/kg - day)} = \text{CS} \times \text{CF}_1 \times \frac{\frac{\text{IR}_C \times \text{EF} \times \text{ED}_C}{\text{BW}_C} + \frac{\text{IR}_A \times \text{EF} \times \text{ED}_A}{\text{BW}_A}}{\text{AT} \times \text{CF}_2} \quad (1)$$

where CS=contaminant concentration in sediment (mg/kg); CF<sub>1</sub>=conversion factor (0.000001 mg/kg); CF<sub>2</sub>=conversion factor (365 days/year); IR<sub>c</sub>=intake rate of child (200 mg/day); IR<sub>A</sub>=intake rate of adult (100 mg/day); EF=exposure frequency (22 days/year); ED<sub>c</sub>=exposure duration of child (6 years); ED<sub>A</sub>=exposure duration of adult (24 years); BW<sub>c</sub>=body weight of child (15 kg); BW<sub>A</sub>=body weight of adult (70 kg), and AT=averaging time (10,950 days).

(ii) Chronic intake from dermal contact with sediments is calculated as follows in Eq. (2) [32]:

$$\text{Intake (mg/kg - day)} = \frac{\text{CS} \times \text{CF} \times \text{SA} \times \text{AF} \times \text{ABS} \times \text{EF} \times \text{ED}}{\text{BW} \times \text{AT}} \quad (2)$$

where CS=contaminant concentration in sediment (mg/kg);CF=conversion factor (0.000001 mg/kg); SA=surface area (1,840 cm<sup>2</sup>); AF=adherence factor (0.95 mg/cm<sup>2</sup>-event); ABS=absorption factor (10.5%); EF=exposure frequency (22 events/year); ED=exposure duration (30 years); BW=body weight (70 kg), and AT=averaging time (10,950 days).

### 2.9. Principal component analysis (PCA)

Data analysis was carried out using SPSS-19. The statistical analysis was used to assess different sources of PAH compounds and how they are being deposited in the Red Sea coast. The statistical analysis was used to elucidate linear combinations of PAHs that may be useful to distinguish between the different possible sources as has been demonstrated by other researches [33,11].

## 3. Results and discussion

### 3.1. Distribution and sources of *n*-alkanes

Table 4 showed the concentrations of *n*-alkanes from C<sub>9</sub> to C<sub>40</sub> and the diagnostic criteria useful for the identification of natural or anthropogenic origins as well as the granulometric parameters of the sediments. The concentrations below their limits of detection were given a value of zero for the calculation. In the present study, the total aliphatic hydrocarbon concentrations varied from 4.23 to 71.87 μg g<sup>-1</sup> (dry weight) with a mean value of 23.02 ± 17.15 μg g<sup>-1</sup>. The highest concentrations occurred at Sharm, Safaga and Marsa Alam stations (71.87, 38.62 and 35.45 μg g<sup>-1</sup>, respectively), while the lowest concentrations were recorded at Salatin 1, Ras Suder and Dahab stations (4.23, 6.73, and 7.78 μg g<sup>-1</sup>, respectively). The present work gave values higher than those detected (0.57–7.8 μg g<sup>-1</sup>) for the Egyptian Mediterranean coast during October 2006

Table 4

Concentrations of *n*-alkanes (μg g<sup>-1</sup>) and calculated distribution indexes in surface sediments of the Red Sea coast

Stations	∑C <sub>9</sub> –C <sub>40</sub>	LMW/HMW	CPI	TAR	P <sub>aq</sub>
1	26.02	0.24	0.93	8.12	0.35
2	25.01	0.22	0.35	2.54	0.12
3	7.781	0.40	0.40	4.22	0.30
4	9.483	0.24	0.41	27.26	0.31
5	15.891	0.51	0.39	2.14	0.39
6	71.874	0.38	0.49	1.52	0.27
7	32.082	0.25	0.42	2.32	0.30
8	6.734	0.29	0.29	5.43	0.43
9	34.140	0.23	0.48	1.75	0.30
10	7.953	0.09	0.77	7.05	0.38
11	15.915	0.15	0.42	19.76	0.29
12	8.472	0.74	0.35	0.62	0.51
13	38.619	0.56	0.50	1.14	0.29
14	18.440	0.49	0.38	0.41	0.38
15	35.445	0.35	0.53	3.10	0.23
16	4.232	0.32	0.48	2.88	0.39
17	33.279	0.15	0.16	3.36	0.34
Mean	23.022	0.33	0.46	5.51	0.33
S.D.	17.145	0.17	0.18	7.22	0.09

LMW/HMW ratio: ∑>C<sub>23</sub>/∑<C<sub>23</sub>. CPI: carbon preference index. TAR: terrigenous/aquatic ratio.

[34]. Also, the presented work showed total aliphatics concentrations higher than those reported for coastal sediments collected during 2005 from Bahrain (0.7–4.4 μg g<sup>-1</sup>), Iran (0.3–1.1 μg g<sup>-1</sup>), Kuwait (0.2–2.7 μg g<sup>-1</sup>), Oman (0.2–1.4 μg g<sup>-1</sup>), Qatar (0.1–4.4 μg g<sup>-1</sup>), Saudi Arabia (0.4–2.3 μg g<sup>-1</sup>), and United Arab Emirates (0.2–1.6 μg g<sup>-1</sup>) [35].

The variation in *n*-alkanes content may refer to the anthropogenic sources (sewage, industrial discharges, and shipping activities) and natural inputs (submerged/floating macrophytes and emergent terrestrial plants and microbial activity) [36]. To assess the possible sources of *n*-alkanes in the Red Sea sediments, two hydrocarbon distribution indexes were calculated: (1) the low molecular weight to high molecular weight ratio (LMW/HMW), and (2) the carbon preference index (CPI). These two indexes have been frequently used as source indicators for *n*-alkanes in marine sediments [37,38].

The LMW/HMW is the concentration ratio of the LMW (∑C<sub>9</sub>–C<sub>23</sub>) to HMW (∑C<sub>23</sub>–C<sub>40</sub>) *n*-alkanes. It has been reported that the LMH/HMW ratios less than 1 usually represent the *n*-alkanes produced by higher plants, marine animals and sedimentary bacteria, while the LMW/HMW ratios close to 1

suggest *n*-alkanes that mainly come from petroleum and plankton sources [39]. The LMW/HMW ratios more than 2 often indicate the presence of fresh oil in sediments [40].

CPI (Eq. (3)) [41] representing the predominance of odd over even *n*-alkanes is:

$$\text{CPI} = \frac{\sum(C_{23} - C_{39})\text{odd}}{2 \sum(C_{24} - C_{40})\text{even}} \quad (3)$$

The CPI of *n*-alkanes is a robust indicator that is used to identify sources of hydrocarbons from vascular plants vs. fossil fuel contamination. *n*-Alkanes contributed from terrestrial vascular plants usually have CPI values ranging from 3 to 6, while petrogenic hydrocarbons show CPI values close to 1 [42,43]. The CPI values of the *n*-alkanes in the studied samples were found to vary from 0.16 to 0.93 in sediments at different locations (Table 4). This finding indicates that only four of the studied locations have CPI value close to 1, which indicates that these four locations are contaminated by petrogenic hydrocarbons [38].

The terrigenous/aquatic ratio (TAR) (Eq. (4)) [44] is defined as:

$$\text{TAR} = \frac{(C_{27} + C_{29} + C_{31})}{(C_{15} + C_{17} + C_{19})} \quad (4)$$

which evaluates the importance of terrigenous inputs versus aquatic inputs. This ratio was below one for Hurghada and Quseir regions (0.60 and 0.41), possibly due to a high bacterial activity or a marine contribution of short *n*-alkanes ( $<C_{23}$ ) [45].  $P_{\text{aq}}$  plant-type ratio [46] quantifying the different plant types in the sea (e. g. submerged vs. emergent) and can be represented by the following Eq. (5):

$$P_{\text{aq}} = \frac{(C_{23} + C_{25})}{(C_{23} + C_{25} + C_{29} + C_{31})} \quad (5)$$

An *n*-alkane proxy ( $P_{\text{aq}}$ ) was proposed by [46], to categorize the sources of submerged and emergent vegetation.  $P_{\text{aq}}$  values for emergent and submerged freshwater vegetation are generally within the range of 0.01–0.23 and 0.48–0.94, respectively [46,47].  $P_{\text{aq}}$  values in the Red Sea sediments ranged between 0.12 and 0.51, which indicated the contribution of both higher plant/macrophyte waxes derived and phytoplankton-derived OC.

The results obtained showed the contribution of both higher plant/macrophyte waxes derived and phytoplankton-derived OC. There was no correlation between (*n*-alkane and TOC%) ( $r=0.002$ ), which

indicated that the changes in *n*-alkane concentration cannot be depended on TOC contents.

### 3.2. Polycyclic aromatic hydrocarbons

Individual and total concentrations of PAHs, as well as characteristic ratios for the identification of PAH origins are given in Tables 5 and 6. Total PAHs ( $\Sigma$ PAHs) concentrations in sediments varied significantly among the studied locations. The values ranged from 0.132 to 5.182  $\mu\text{g g}^{-1}$ , with an average 1.628  $\pm 1.477 \mu\text{g g}^{-1}$ . The highest concentration of the total PAHs is recorded in sediments collected from Ras Suder (5.182  $\mu\text{g g}^{-1}$ ), followed by that in El-Tour (4.052  $\mu\text{g/g}$ ), Sharm (3.367  $\mu\text{g g}^{-1}$ ), Quseir (2.888  $\mu\text{g g}^{-1}$ ), Taba (2.233  $\mu\text{g g}^{-1}$ ) and Hurghada (1.631  $\mu\text{g g}^{-1}$ ). Low concentrations were detected in Ras Gharib, Shalatin 1 and Na'ama Bay (0.132, 0.179, and 0.279  $\text{ng g}^{-1}$ , respectively). The variability in PAHs content along the Red Sea sediments may be attributed to the different sources of discharged waters and proximity to human activities and fuel combustion emissions. The concentrations of PAHs in sediments were affected by the chemical composition of the sediments such as organic matter, clay, and sand [34,48].

Sediments with high organic carbon content were characterized with high values of PAHs [23,49]. According to the present data, no correlation ( $R^2=0.045$ ) was found between  $\Sigma$ PAHs and TOC% concentrations in the Red Sea sediments. The same result was observed by Viñas et al. [50] and de More et al. [35] in different polluted areas.

Also, the absence of a correlation between total hydrocarbons and PAHs ( $R^2=0.102$ ) indicated different primary sources and/or different transport processes for the two classes of compounds. Also the same lack of correlation was reported in offshore sediment from the Black Sea [21,51]. According to the classification suggested by Baumard et al. [20] and Mostafa et al. [52], the concentration of PAHs in sediments can be considered as low  $\Sigma$ PAH (between 0.0 and 0.10  $\mu\text{g g}^{-1}$ ), moderate  $\Sigma$ PAH (between 0.10 and 1.0  $\mu\text{g g}^{-1}$ ), high  $\Sigma$ PAH (between 1.0 and 5.0  $\mu\text{g g}^{-1}$ ), and very high  $\Sigma$ PAH concentrations (above 5.0  $\mu\text{g g}^{-1}$ ). In this study, the highest value found was at Ras Suder (5.182  $\mu\text{g g}^{-1}$ ), which classifies this sampling point as very high levels of pollution [16]. According to the total PAHs recorded in the studied locations, the sediments collected from stations 3, 4, 9, 10, 11, 13, and 16 can be considered as moderately polluted, while the sediments collected from stations 1, 2, 5, 6, 7, 12, 14, 15, and 17 can be considered as highly

Table 5  
Concentrations ( $\mu\text{g g}^{-1} \times 10^{-3}$ ) of individual PAHs in sediments collected from the Egyptian Red Sea coast

PAHs	1	2	3	4	5	6	7	8	9	10	11	12	13	14	15	16	17	Mean	SD
Naph	n.d.	n.d.	n.d.	4	n.d.	n.d.	n.d.	n.d.	3	n.d.	4	n.d.	3	n.d.	n.d.	1	4	1.1	1.7
Acthy	14	9	n.d.	11	n.d.	n.d.	8	40	2	21	12	2	14	17	21	n.d.	5	10.9	10.2
Ace	80	42	n.d.	17	75	39	38	211	14	21	16	75	26	50	33	2	49	46.4	48.9
Fl	45	35	5	17	43	66	22	330	11	24	15	28	38	41	15	2	13	44.1	75.5
Phe	450	157	3	10	109	123	91	300	11	36	11	57	81	117	6	12	16	93.5	119.7
Ant	61	79	60	11	116	292	92	191	28	108	8	122	61	558	69	17	32	112.1	135.2
Flu	406	333	61	3	153	747	390	257	24	114	1	45	219	598	66	3	276	217.1	220.4
Pyr	111	361	84	67	340	809	352	338	39	122	3	81	115	592	81	29	367	228.9	223.7
BaA	1,027	111	37	n.d.	30	231	863	1,154	25	44	46	1,152	64	150	35	10	229	306.4	434.2
Chr	12	39	24	39	691	909	2077	2,300	83	234	11	12	27	640	983	12	135	484.0	723.9
BbF	6	32	7	n.d.	9	39	43	13	10	7	n.d.	14	29	25	10	10	91	20.3	22.4
BkF	12	88	17	n.d.	12	66	39	25	19	11	n.d.	30	42	53	18	37	21	28.8	23.4
BaP	3	25	7	15	7	14	11	7	10	3	n.d.	3	17	14	10	5	11	9.5	6.3
DBA	1	1	n.d.	3	4	3	5	2	11	n.d.	1	2	10	5	2	14	5	4.1	4.0
Bghip	2	8	1	63	9	23	16	7	17	2	3	4	23	13	4	13	11	12.9	14.7
InP	3	12	6	19	6	6	5	7	6	5	1	4	10	15	7	12	5	7.6	4.6
$\Sigma$ PAHs	2,233	1,332	312	279	1,614	3,367	4,052	5,182	313	752	132	1,631	779	2,888	1,360	179	1,270	1,628	148

Naph = naphthalene, Acthy = acenaphthylene, Ace = acenaphthene, Fl = fluorene, Phe = phenanthrene, Ant = anthracene, Flu = fluoranthene, Pyr = pyrene, BaA = benzol[anthra]cene, Chr = chrysene, BbF = benzo[b]fluoranthene, BkF = benzo[k]fluoranthene, BaP = benzo[a]pyrene, DBA = dibenzol[a,h]anthracene, Bghip = benzo[ghi]perylene, InP = indeno[1,2,3-cd]pyrene,  $\Sigma$ PAHs = total PAHs in sediment.

Table 6  
Total hydrocarbons (TH,  $\mu\text{g/g}$ ), pyrolytic ( $\sum\text{COMB}$ ,  $\mu\text{g/g}$ ), fossil ( $\sum\text{PAE}$ ,  $\mu\text{g/g}$ ),  $\sum\text{COMB}/\sum\text{PAHs}$  (C/P),  $\sum\text{LP-PAHs}/\sum\text{PH-PAHs}$ : concentration ratio of sum of 6 three-ring PAHs to sum of more than three-ring PAHs

Site no.	TH	$\sum\text{COMB}$	$\sum\text{COMB}/\sum\text{PAHs}$	$\sum\text{PHE}$	$\sum\text{LP-PAHs}$	$\sum\text{HP-PAHs}$	PAH <sub>Carc</sub>	% CARC	Phen/Ant	Flu/(Flu + Phe)	Flu/(Flu + Py)	IcdB/(IcP + Bghip)
1	29.625	1.583	0.71	0.650	0.41	1.066	47.74	7.38	0.47	0.79	0.60	0.60
2	27.653	1.010	0.76	0.322	0.32	0.316	23.72	1.99	0.68	0.48	0.60	0.60
3	8.499	0.244	0.78	0.068	0.28	0.099	31.73	0.05	0.95	0.42	0.86	0.86
4	10.257	0.209	0.75	0.070	0.36	0.139	49.82	0.91	0.23	0.04	0.23	0.23
5	18.352	1.261	0.78	0.353	0.28	0.768	47.58	0.94	0.58	0.31	0.40	0.40
6	79.194	2.846	0.85	0.520	0.18	1.291	38.34	0.42	0.86	0.48	0.20	0.20
7	37.910	3.799	0.94	0.251	0.07	3.057	75.48	0.99	0.81	0.53	0.24	0.24
8	12.269	4.117	0.79	1.072	0.26	3.522	67.87	1.57	0.46	0.43	0.50	0.50
9	36.272	0.244	0.78	0.069	0.28	0.181	57.83	0.39	0.69	0.38	0.26	0.26
10	9.114	0.542	0.72	0.210	0.39	0.306	40.69	0.33	0.76	0.48	0.71	0.71
11	16.921	0.067	0.50	0.068	1.02	0.063	46.67	1.38	0.08	0.25	0.25	0.25
12	10.551	1.347	0.83	0.284	0.21	1.221	74.86	0.47	0.44	0.36	0.50	0.50
13	41.418	0.556	0.71	0.223	0.40	0.222	28.50	1.33	0.73	0.66	0.30	0.30
14	22.679	2.105	0.73	0.783	0.37	0.915	31.68	0.21	0.84	0.50	0.54	0.54
15	38.736	1.216	0.89	0.144	0.12	1.069	78.60	0.09	0.92	0.45	0.64	0.64
16	4.618	0.145	0.81	0.034	0.23	0.113	63.13	0.71	0.20	0.09	0.48	0.48
17	36.324	1.151	0.91	0.119	0.10	0.508	40.00	0.50	0.95	0.43	0.31	0.31

polluted (Table 5). Table 7 lists worldwide concentrations of total aliphatic and PAHs in coastal sediments.

3.3. Calculation for carcinogenic PAHs ( $\Sigma\text{PAH}_{\text{CARC}}$ ) in sediment samples

Eight PAHs (Car-PAHs) typically considered as possible carcinogens are: benzo(a)anthracene, chrysene, benzo(b)fluoranthene, benzo(k)fluoranthene, benzo(a)pyrene, dibenzo(a,h)anthracene, indeno(1,2,3-cd)pyrene and benzo(a,h,i)perylene [60,61]. In particular, benzo(a)pyrene has been identified as being highly carcinogenic [62,63]. The US Environmental Protection Agency (EPA) has promulgated 16 unsubstituted PAHs (EPA-PAH) as priority pollutants [64].

Table 7  
Worldwide concentrations of total hydrocarbons in sediments ( $\text{ng g}^{-1}$  dry wet)

Site	Concentration range ( $\mu\text{g g}^{-1}$ dry wet)	References
Red Sea coast	0.132–5.182	Present work
Western Mediterranean	0.180–3.200	[53]
Baltic Sea	0.720–1.900	[49]
Baltic Sea	0.005–22.10	[54]
Cretan Sea (South Aegean Sea)	0.015–0.159	[55]
Black Sea	0.014–0.368	[21]
Ukraine, Black Sea	0.007–0.64	[21]
Marmara Sea (Turkey)	0.120–11.40	[56]
Marmara Sea (Turkey)	0.05–13.482	[57]
Mediterranean	0.088–6.338	[58]
Mediterranean	0.45–44.490	[34]
Marmara Sea	0.144	[59]

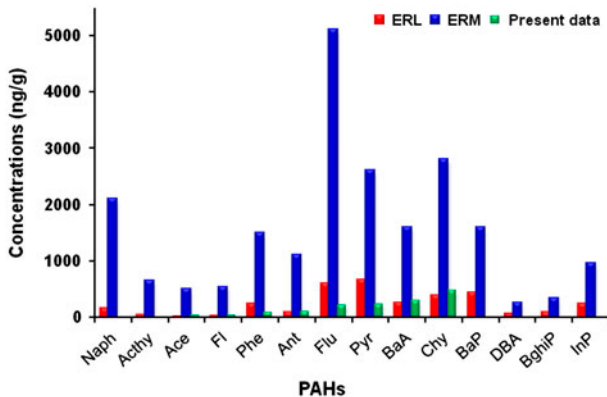


Fig. 2. Diagram showed the average concentrations ( $\text{ng/g}$  dry wet) of the individual PAH in the Red Sea sediments relative to ERL and ERM.

The highest value of the eight carcinogenic PAHs ( $\Sigma\text{PAH}_{\text{CARC}}$ ) was recorded at Ras Suder ( $3.522 \mu\text{g g}^{-1}$ ), while the highest  $\Sigma\text{PAH}_{\text{CARC}}$  percentage (CARC% = 78.6%) was recorded at Marsa Alam station. Ras Suder (67.87%), El Tour (75.48), Hurghada (74.86), Marsa Alam (78.60) and Shalatin-1 (63.13) reported high carcinogenic PAHs percentage. This indicates the adverse effect of sediments at Ras Suder, Hourghada, El Tour and Marsa Alam stations on the human health. The carcinogenic benzo(a)anthracene was very high at Taba, El Tour, Ras Suder and Hurghada stations, while the second carcinogenic PAH chrysene was very high at Ras Mohamed, Sharm, El Tour, Ras Suder, Quseir and Marsa Alam stations.

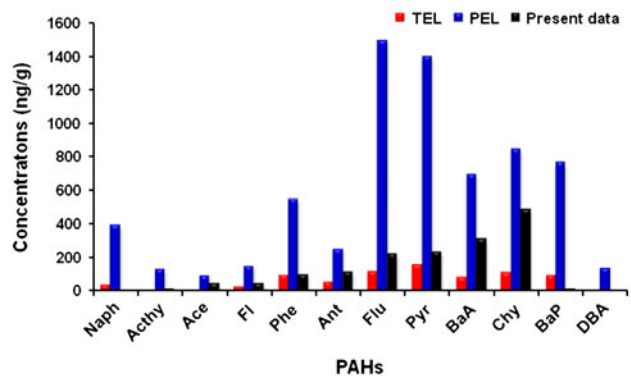


Fig. 3. Diagram showed the average concentrations ( $\text{ng/g}$  dry wet) of the individual PAH in the Red Sea sediments relative to TEL and PEL.

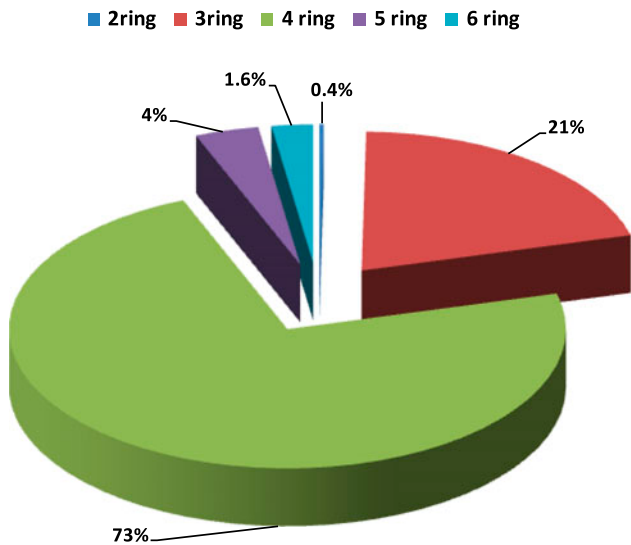


Fig. 4. Percentage of individual PAH to the total PAHs in the Red Sea sediments.

Table 8  
Diagnostic ratios between PAHs in the Egyptian surface coastal Red Sea sediments

Locations	St. no.	D-1	D-2	D-3	D-4	D-5	D-6
Taba	1	0.60	0.79	0.20	0.88	0.50	0.12
Nuweiba	2	0.60	0.48	0.39	0.67	0.36	0.34
Dahab	3	0.86	0.42	0.23	0.05	0.41	0.95
Na'ama Bay	4	0.23	0.04	0.28	0.48	N.D.	0.52
Ras Mohamed	5	0.40	0.31	0.01	0.48	0.75	0.52
Sharm	6	0.20	0.48	0.02	0.30	0.59	0.70
El Tour	7	0.24	0.53	0.01	0.50	1.10	0.50
Ras Suder	8	0.50	0.43	0.01	0.61	0.52	0.39
Suez	9	0.26	0.38	0.11	0.28	0.53	0.72
Ain Sukhna	10	0.71	0.48	0.01	0.25	0.64	0.75
Ras Gharib	11	0.25	0.25	N.D	0.58	N.D	0.42
NIOF HU	12	0.50	0.36	0.20	0.32	0.47	0.68
Safaga	13	0.30	0.66	0.39	0.57	0.69	0.43
Quseir	14	0.54	0.50	0.02	0.17	0.47	0.83
Marsa Alam	15	0.64	0.45	0.01	0.08	0.56	0.92
Shalatin-1	16	0.48	0.09	0.29	0.41	0.27	0.59
Shalatin-2	17	0.31	0.43	0.08	0.33	4.33	0.67

D-1 = InP/(InP + BghiP); D-2 = Flu/(Flu + Pyr); D-3 = BaP/(BaP + Chr); D-4 = Phe/(Phe + Ant); D-5 = BbF/BkF; D-6 = Ant/(Ant + Phe); NA = not available.

### 3.4. Classification of sediments according to sediment quality criteria

Two widely used sediment quality guidelines, the effects range-low (ERL) and effects range median (ERM) value guidelines [65,66] as well as the threshold effects level (TEL) and probable effects level (PEL) guidelines [67] were applied to evaluate the possible ecotoxicological risks of PAHs in the studied area. The measured concentrations of PAHs were compared with the ERL, ERM, TEL, and PEL values. The average PAHs content in all studied sediments were lower than the ERM value (44,792 ng g<sup>-1</sup>). The total PAH concentrations recorded in the present study were much lower than the total ERM values (Fig. 2). On the other hand, similar observations were found relative to the TEL and PEL (0.655 and 6.676 µg g<sup>-1</sup>, respectively) for the total PAH [68] (Fig. 3). The concentration levels of Ace, Fl, Phe, Ant, Flu, Pyr, BaA, and Chr were higher than TEL values. These findings indicated that the studied sediments may represent a potential biological impact [69].

### 3.5. The PAH composition pattern

The PAH composition pattern is helpful to track the contaminant source and illustrate the fate and transport of PAHs in multimedia environment [70]. Different sources of PAHs have different PAHs

patterns. Anthropogenic PAHs are formed mainly via two mechanisms: incomplete combustion of fossil fuels and the discharge of petroleum-related materials. The petroleum-derived residues contain relatively higher concentrations of two- and three-ring PAH compounds such as Nap, Ph, and Ant [71]. At low to moderate temperature, as in the wood stove [72]), or as from the combustion of coal [73] low-molecular-weight parent PAH compounds are abundant. At high temperature, the high-molecular-weight parent PAH compounds are dominant [74]. Therefore, on account of the anthropogenic source, the low-molecular-weight parent of PAHs has both petrogenic and combustion (low-temperature pyrolysis) sources, whereas the high

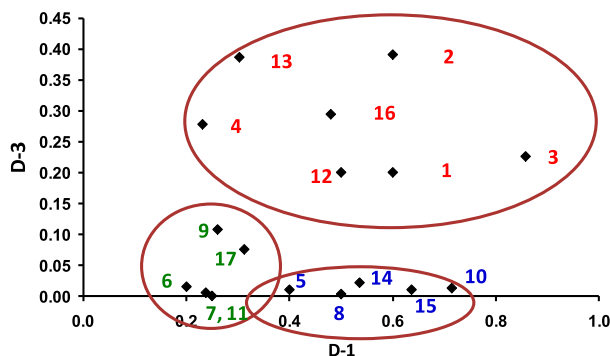


Fig. 5. Plot between D-1 vs. D-3.

Table 9

Factor loadings (varimax normalized: marked loadings are >0.70) for four principal components (PCs) for non-contaminated and for fairly contaminated areas

PAH	PCF1	PCF2	PCF3	PCF4
Naph	-0.616	0.057	0.371	0.525
Acthy	0.570	-0.384	0.517	-0.117
Ace	<b>0.821</b>	-0.350	0.289	0.188
Fl	<b>0.766</b>	-0.279	0.440	0.134
Phe	<b>0.723</b>	-0.214	0.026	-0.014
Ant	<b>0.613</b>	0.429	-0.059	-0.361
Flu	<b>0.691</b>	<b>0.569</b>	-0.250	0.032
Pyr	<b>0.656</b>	<b>0.636</b>	-0.171	0.056
BaA	<b>0.653</b>	-0.409	-0.066	0.267
Chr	<b>0.728</b>	-0.074	0.207	0.169
BbF	0.188	0.527	-0.269	0.689
BKF	0.390	<b>0.734</b>	-0.214	-0.083
BaP	0.097	<b>0.819</b>	0.270	-0.004
DBA	-0.340	0.330	0.189	0.313
Bghip	-0.274	0.445	<b>0.686</b>	0.088
lnP	-0.128	0.580	<b>0.659</b>	-0.332
% of variance	32.07	22.58	12.23	7.98
Cumulative %	32.07	54.65	66.89	74.86

Note: Extraction method: PCA.

Rotation method: Varimax with Kaiser normalization.

molecular parent of PAHs is predominantly pyrogenic [75]. As presented in Fig. 4, high-molecular-weight PAHs with four rings are predominated (73% of the total PAHs) in the sediment samples. The PAHs with three rings were reported 21% of the total PAHs, while the PAHs with the two, five, and six rings were

reported only 6% of the total PAHs in the studied sediment samples. These results can be explained as the total PAHs in the studied sediment samples may have come from a pyrogenic source.

### 3.6. Possible sources of PAHs in the studied locations

It is possible to classify the contaminant sources as either petrogenic or pyrolytic using the ratios between some individual PAHs in the sediments. The use of ratios is based on the temperature of the formation of PAHs, taking into account the individual chemical stabilities [16]. Pyrogenic (e.g. fossil fuel combustion and vegetation fires) and petrogenic (e.g. oil spill and petroleum products inputs) are the primary sources of PAHs found in coastal marine sediments [73,76]. To assess the main source of PAHs in the Red Sea sediments, some calculated PAH distribution indexes such as the ratio of  $\sum PL_{PAHs}/\sum PH_{PAHs}$  (sum of two and three rings PAHs to the sum of more than three rings PAHs) and the ratio of phenanthrene to anthracene (Phen/Ant).

Studies have shown that high  $\sum PL_{PAHs}/\sum PH_{PAHs}$  ratios (>1) often indicate PAHs with petrogenic predominate sources, while low  $\sum PL_{PAHs}/\sum PH_{PAHs}$  ratios suggest PAHs of pyrolytic origin [19,38,77]. The data of  $\sum PL_{PAHs}/\sum PH_{PAHs}$  reported in Table 6 showed that Ras Gharib station is the only site that has a value more than 1, which indicated petrogenic origin. As for Phen/Ant ratios, PAHs from petrogenic sources usually have values larger than 15 and less than 10 when they are of a pyrolytic origin [7,38,78].

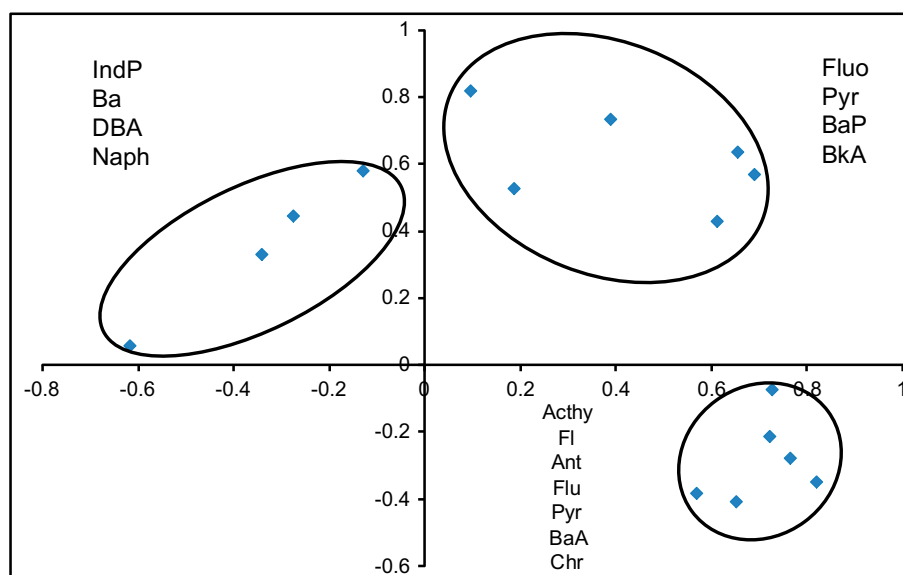


Fig. 6. Score plot of PCF1 vs. PCF2 illustrating the distribution of individual PAH compounds in the Red Sea sediments.

Table 10  
Correlation coefficient matrix for Red Sea sediment individual PAHs and  $\Sigma$ PAHs and TOC%

	(Naph)	(Achy)	(Ace)	(Fl)	(Phe)	(Ant)	(Flu)	(Pyr)	(BaA)	(Chr)	(BbF)	(BkF)	(BaP)	(DBA)	(Bghip)	(InP)	$\Sigma$ PAHs)	% TOC			
(Naph)	1.000																				
(Achy)	-0.173	1.000																			
(Ace)	-0.324	0.691**	1.000																		
(Fl)	-0.248	0.738**	0.915**	1.000																	
(Phe)	-0.414	0.439	0.674**	0.556*	1.000																
(Ant)	-0.449	0.226	0.277	0.271	0.227	1.000															
(Flu)	-0.382	0.049	0.246	0.217	0.498*	0.714**	1.000														
(Pyr)	-0.349	0.021	0.281	0.277	0.253	0.738**	0.899**	1.000													
(BaA)	-0.378	0.295	0.715**	0.540*	0.654**	0.111	0.236	0.089	1.000												
(Chr)	-0.414	0.544*	0.624**	0.67**	0.292	0.332	0.366	0.447	0.470	1.000											
(BbF)	0.173	-0.208	0.031	-0.054	-0.066	0.120	0.482*	0.539*	0.059	0.143	1.000										
(BkF)	-0.384	-0.175	0.019	0.061	0.150	0.452	0.636**	0.633**	0.016	0.126	0.411	1.000									
(BaP)	0.054	-0.069	-0.114	-0.039	-0.035	0.203	0.400	0.444	-0.289	0.029	0.404	0.705**	1.000								
(DBA)	0.326	-0.322	-0.264	-0.178	-0.265	-0.095	-0.119	-0.112	-0.258	-0.116	0.142	0.149	0.141	1.000							
(Bghip)	0.495*	-0.125	-0.206	-0.092	-0.216	-0.057	-0.009	0.059	-0.247	-0.061	-0.002	-0.045	0.452	0.264	1.000						
(InP)	0.130	0.046	-0.153	-0.040	-0.155	0.248	0.032	0.104	-0.359	-0.108	-0.076	0.278	0.624**	0.290	0.700**	1.000					
$\Sigma$ PAHs)	-0.519	0.479	0.757**	0.716**	0.601*	0.558	0.678**	0.663	0.685**	0.867**	0.267	0.339	0.094	-0.206	-0.116	-0.118	1.000				
% TOC	0.422	0.044	-0.121	-0.046	-0.094	-0.237	-0.207	-0.263	-0.110	-0.129	-0.141	-0.278	-0.402	-0.126	-0.278	-0.426	-0.214	1.000			
TH	-0.001	-0.204	-0.080	-0.058	0.110	0.222	0.668**	0.603*	-0.042	0.207	0.502*	0.456	0.421	0.109	0.118	-0.180	0.320	-0.062			

\*Correlation is significant at the 0.05 levels (2-tailed).

\*\*Correlation is significant at the 0.01 levels (2-tailed).

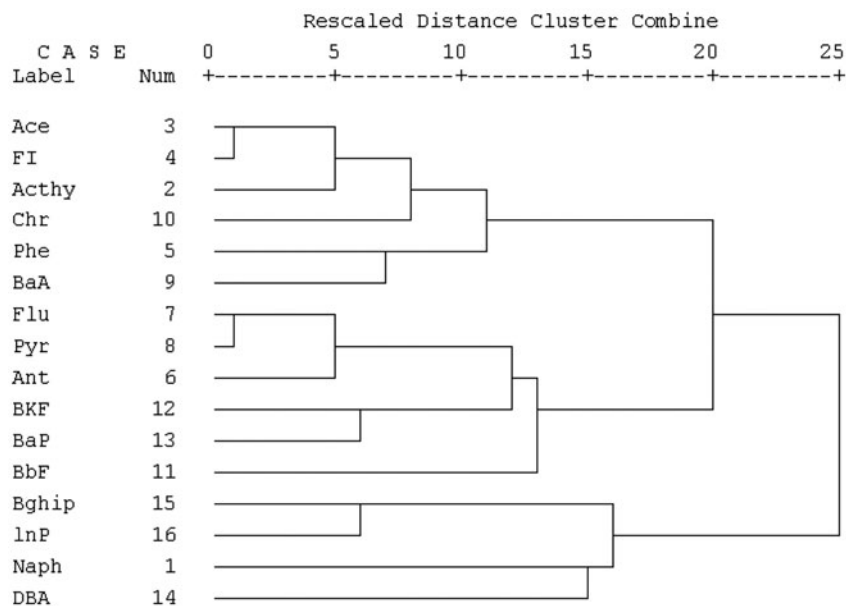


Fig. 7. Hierarchical dendrogram for 16 PAHs represented by Ward's hierarchical clustering method.

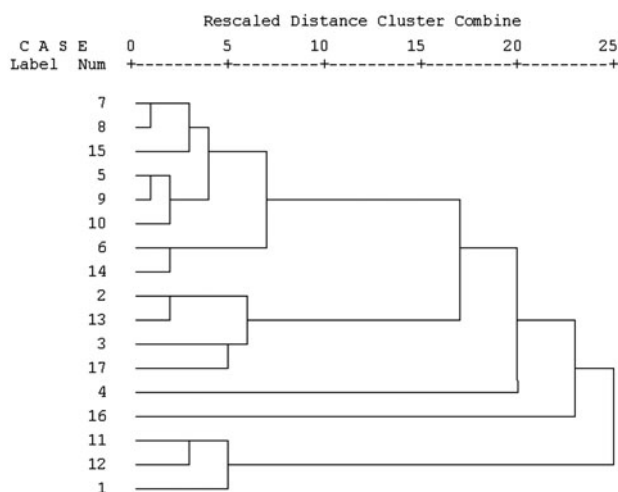


Fig. 8. Hierarchical dendrogram for 17 sampling locations represented by Ward's hierarchical clustering method.

Further discrimination of PAH sources can be achieved using the ratios of other isomers. IcdP/(BghiP+IcdP) ratio is used in this study, and values for this ratio greater than 0.5 are also due to petrogenic origins. The Flu/(Flu+Py) ratio is <0.5 for petrogenic sources and >0.5 for pyrogenic PAH sources.

Table 6 shows the ratios obtained from the studied sediments. By comparing these data, it was possible to extract some information that is important to consider. In this case,  $\sum PL_{PAHs} / \sum PH_{PAHs}$  ratios ranged from 0.07 to 1.02; most of the location had low values (<1),

which confirmed a suspected pyrogenic input. In all of the studied sites, the Phen/Ant indices were less than 10, which also indicated important pyrogenic sources. IcdP/(BghiP+IcdP) indices for the present samples ranged from 0.20 to 0.71, which again indicated pyrogenic sources. The Flu/(Flu+Py) ratio ranged from 0.04 to 0.79, and this fact indicated that the contamination may have occurred due to both petrogenic and pyrolytic sources. However, by analyzing the results in Table 6, it can be suggested that the PAHs detected in the studied sediment samples may be due to contributions of both pyrolytic and petrogenic sources, but the majority was from the pyrolytic sources.

The ratio of the sum of major combustion-specific compounds ( $\Sigma COMB = Flu, Pyr, BaA, Chr, BbF, BkF, BaP, InP, \text{ and } BghiP$ ) to the sum of 16 EPA-PAHs ( $\Sigma COMB / \Sigma PAHs$ ) ranged from 0.50 to 0.94, and the  $\Sigma COMB$  concentrations displayed values from 67 to 4,117 ng g<sup>-1</sup> (Table 6). The highest ratio (0.94) was detected at station 7 and indicated that the PAHs at this site mainly came from combustion origin. The high  $\Sigma COMB / \Sigma PAHs$  ratio values further indicated that extensive combustion activities affected the PAHs in sediment samples along the Egyptian Red Sea coast.

Other six diagnostic ratios between individual PAH concentrations were calculated and used to make the identification of the PAHs origin more precisely (Table 8): D-1 = InP/(InP+BghiP); D-2 = Flu/(Flu+Pyr); D-3 = BaP/(BaP+Chr); D-4 = Phe/(Phe+Ant),

Table 11

Chronic daily intake and dermal contact of individual hydrocarbons compounds and total hydrocarbons of sediment from the Red Sea coast

PAHs	Intake (mg kg <sup>-1</sup> dw)	Dermal (mg kg <sup>-1</sup> dw)	ISQG-Low (Trigger value)*(mg kg <sup>-1</sup> dw)	ISQG-high*(mg kg <sup>-1</sup> dw)
Naph	7.03092E-10	2.930E-04	160	2,100
Acthy	6.8829E-09	2.869E-03	44	640
Ace	2.91598E-08	1.215E-02	16	500
Fl	2.77536E-08	1.157E-02	19	540
Phe	5.88377E-08	2.452E-02	240	1,500
Ant	7.04943E-08	2.938E-02	85	1,100
Flu	1.3677E-07	5.701E-02	600	5,100
Pyr	1.43986E-07	6.001E-02	665	2,600
BaA	1.92721E-07	8.033E-02	261	1,600
Chr	3.04476E-07	1.269E-01	384	2,800
BbF	1.27667E-08	5.321E-03		
BkF	1.81324E-08	7.558E-03		
BaP	5.99479E-09	2.499E-03	430	1,600
DBA	2.55334E-09	1.064E-03	63	260
Bghip	8.10406E-09	3.378E-03		
InP	4.77363E-09	1.990E-03		
Max	3.04476E-07	1.269E-01		
Min	7.03092E-10	2.930E-04		
Mean	6.401E-08	2.668E-02		
S.D	8.735E-08	3.641E-02		

D-5 = BbF/BkF and D-6 = Ant/(Ant + Phe) [34,79]. D-1 ratio is less than 0.4 for petroleum and >0.5 for petroleum/combustion mixture. Literature values of D-1 ratio are above 0.5 for grass combustion, wood soot, and creosote [80]. D-3 ratio values are less than 0.2 for combustion and between 0.6 and 0.9 for petroleum, while ratios between 0.4 and 0.6 are due to a petroleum/combustion mixture. D-6 ratio <0.1 is usually taken as an indication of petroleum, while a ratio >0.1 indicates a dominance of combustion [19]. D-6 ratios >0.1 represent the combustion of diesel oil, shale oil, coal and some crude oil samples. D-2 ratio of 0.4 is usually defined as petroleum, while ratio of 0.5 is for the petroleum/combustion transition point, however, this boundary appears to be less definitive than 0.1 for D-6. Generally, the D-2 ratio is below 0.4 for most petroleum samples and above 0.5 in kerosene, grass, most coal, and wood combustion samples and creosote, but ratio between 0.4 and 0.5 is a characteristic of liquid fossil fuel such as gasoline, diesel, fuel oil, and crude oil combustion and emissions from cars and diesel trucks. Eight diagrams were plotted to clarify the results obtained from the above ratios. These diagrams gave three groups indicating three sources; the first

represented the stations of petrogenic sources, the second group represented the stations of pyrogenic sources (most stations), and the third group represented the stations of a mixture of petrogenic and pyrogenic sources. Plot of D-1 vs. D-3 divided the location to three groups: the first group contains 1, 2, 3, 4, 12, 13, and 16 stations; the second group contains 6, 7, 9, 11, and 17; and the third group contains 5, 8, 10, 14, and 15 (Fig. 5).

### 3.7. Risk assessment

Tables 11 and 12 demonstrate the chronic daily intake and dermal contact with contaminated sediment values of total hydrocarbons and individual PAH compounds along the Red Sea coast of Egypt. The present results of the Red Sea sediment were compared with the Interim Sediment Quality Guidelines (ISQGs), which contain two concentrations, the ISQG-Low concentration (or trigger value) and the ISQG-High concentration. The trigger value is a threshold concentration, and below this concentration, the frequency of adverse effects is expected to be very low. The ISQG-High concentration is intended to

Table 12  
Chronic daily intake and dermal contact of total hydrocarbons of sediment from the Red sea coast

Station	$\sum$ PAHs** Intake (mg kg <sup>-1</sup> dw)	$\sum$ PAHs** Dermal (mg kg <sup>-1</sup> dw)
1	1.40474E-06	5.855E-01
2	8.37938E-07	3.493E-01
3	1.96274E-07	8.181E-02
4	1.75514E-07	7.315E-02
5	1.01534E-06	4.232E-01
6	2.11812E-06	8.828E-01
7	2.54904E-06	1.062E+00
8	3.25991E-06	1.359E+00
9	1.96903E-07	8.207E-02
10	4.7307E-07	1.972E-01
11	8.30389E-08	3.461E-02
12	1.02603E-06	4.276E-01
13	4.90055E-07	2.043E-01
14	1.81679E-06	7.572E-01
15	8.55552E-07	3.566E-01
16	1.12606E-07	4.693E-02
17	7.98935E-07	3.330E-01
Max	3.25991E-06	1.359E+00
Min	8.30389E-08	3.461E-02
Mean	1.02411E-06	4.268E-01
S.D	9.28815E-07	3.871E-01

Note: The values are extracted from Australian interim sediment quality guideline (ISQG) values [81].

\*\*The ISQG-Low and ISQG-high values for the total hydrocarbons are (4,000 and 45,000, respectively).

Interim Sediment Quality Guidelines—Low: Probable effects concentrations below which biological effects would rarely occur. Interim Sediment Quality Guidelines—High: Probable effects concentrations below which biological effects would possibly occur.

Concentrations above these values represent a probable-effects range within which effects would be expected to frequently occur.

represent a concentration above which the adverse biological effects are expected to occur more frequently. In the present study, both of the total PAHs and individual PAH compounds were less than the trigger values of ISQGs for all studied stations which indicated that no health effect may occur due to the intake and dermal contact with the studied sediment samples [65,66].

### 3.8. Principal component analysis

Data submitted for the PCA analysis were arranged in a matrix, where each column corresponds to one of the PAH component and each row represents one location. The number of factors extracted

from the variables was determined according to Kaiser's rule, which retains only factors with eigenvalues that exceed one. The first step in the multivariate statistical analysis was the application of PCA with the aim to group the individual PAH components by the loading plots for 17 contaminated sites. Since the raw data have provided negative loadings, the VARIMAX rotation for the correlation greater than 0.30 were applied. Concentrations of 16 EPA-PAHs as active variables and 17 sites were selected. The majority of the variance (74.86%) of the scaled data was explained by four eigenvectors/principal component factors (PCF). The first principal component factor (PCF1) explained 32.07%, the second (PCF2) explained 22.58%, the third (PCF3) explained 12.23%, and the fourth (PCF4) explained 7.98%. PCF1 had a significant correlation with Ace (0.821), Fl (0.766), Phe (0.723), and Chr (0.723) (Table 9). Thus, PCF1 is a quantitative correlation component and corresponds to the total PAHs concentration. The compounds of Phe and Pyr are components of fossil fuels, and a portion of them is associated with their combustion. Thus, it can be seen that PCF1 reflected the effects of traffic pyrolysis or combustion on the sum of PAHs. PCF2 is dominated by BKF (0.734) and BaA (0.82) which is also associated with traffic emission. The property of individual PAH components, which causes their dominance in each factor can be clearly indicated and their clustering was observed from the PCF1 and PCF2 plot (Fig. 6). The strong adsorption of PAHs by sediments caused by long-range atmospheric transport processes and regional fallout deposition in combination with their transformation, behavior in sediment-water system and mobility imply the random distribution.

The correlations between the individual PAHs, TOC%, and TH are illustrated in Table 10. This statistical approach is based on the fact that each pollution source produces a characteristic PAH pattern; so, the correlations of all the individual PAHs can give an idea on whether they all originate from the same source or not. The total PAHs were correlated with Ace (0.757), Fl (0.716), Phe (0.601), Flu (0.678), BaA (0.685), and Chr (0.867), where TH was correlated with Flu (0.668), Pyr (0.603), and BbF (0.502).

Hierarchical cluster analysis (Ward's method applying Pearson correction) of PAHs components using average linkage between groups and square Euclidean distance and standard deviation <1 showed a good efficiency for sediment samples collected from the Egyptian Red Sea coast, which present different sources deposition (Figs. 7 and 8). Three big clusters with subgroups could be distinguished, which

coincide with the previously defined factor analysis and plot between D-1 and D-3. The first group in the cluster was contained by Ace, Fl, Achy, Chr, Phe, and BaA. The second group was represented by Flu, Pyr, Ant, BkF, BaP, and BbF (Fig. 7). The third group was represented by BghiP, IndP, Naph, and DBA. The linkage distance between classes is high (15.0–20.0) implying a significant distance between them. Statistically sufficient numbers of data can explain the obtained high values for linkage distance. Fig. 8 shows the cluster analysis of the 17 sampling locations, which is explained by three major groups. The first group was represented by eight stations (7, 5, 6, 8, 9, 10, 14, and 15), while the second group was represented by four stations (2, 3, 13, and 17). The third group was represented by only three stations (1, 11, and 12), and the remaining two stations were represented in separated clusters. Most of statistical done on the data obtained were arranged the analysis data in three groups.

#### 4. Conclusion

The detailed study of aliphatic (*n*-alkanes) and PAHs was investigated in surface sediments of the Egyptian Red Sea coast. The distribution of both of *n*-alkanes and PAHs showed great variations in the studied sediment samples. By examining the distribution indexes, it was confirmed that the aliphatic hydrocarbons were mainly from petroleum contamination, while the distribution of PAHs came from both pyrolytic and petrogenic sources. The four rings hydrocarbons were predominated in the sediment samples presenting 73%. The human risk assessment calculation showed that there is no health effect may occur due to the PAHs contaminated in the studied samples.

#### References

- [1] K. Ravindra, R. Sokhi, R. Van Grieken, Atmospheric polycyclic aromatic hydrocarbons: Source attribution, emission factors and regulation, *Atmos. Environ.* 42(13) (2008) 2895–2921.
- [2] J.P. Essien, S.I. Eduok, A.A. Olajire, Distribution and ecotoxicological significance of polycyclic aromatic hydrocarbons in sediments from Iko River estuary mangrove ecosystem, *Environ. Monit. Assess.* 176 (2011) 99–107.
- [3] N.J. Hu, X.F. Shi, P. Huang, J.H. Liu, Polycyclic aromatic hydrocarbons in surface sediments of Laizhou Bay, Bohai Sea, China, *Environ. Earth Sci.* 63 (2011) 121–133.
- [4] E.R. Christentser, S. Arora, Source apportionment of PAHs in sediments using factor analysis by time records. Application to Lake Michigan, USA, *Water Res.* 41 (2007) 168–176.
- [5] B.O. Ekpo, O.E. Oyo-Ita, D.R. Oros, B.R.T. Simoneit, Distributions and sources of polycyclic aromatic hydrocarbons in surface sediments from the Cross River estuary, S.E. Niger Delta, Nigeria, *Environ. Monit. Assess.* 184(2) (2011) 1037–1047.
- [6] T.A.T. Aboul-Kassim, B.R.T. Simoneit, Aliphatic and aromatic hydrocarbons in particulate fallout of Alexandria, Egypt. Sources and implications, *Environ. Sci. Technol.* 29 (1995) 2473–2482.
- [7] P. Baumard, H. Budzinski, Q. Michon, P. Garrigues, T. Burgeot, J. Bellocq, Origin and bioavailability of PAHs in the Mediterranean Sea from mussel and sediment records. *Estua. Coast. Shelf. Sci.* 47 (1998) 77–90.
- [8] A. El Nemr, A. El-Sikaily, A. Khaled, Distribution patterns and risk assessment of hydrocarbons in bivalves from Egyptian Mediterranean coast, *Blue Biotechn. J.* 1(2) (2012) 457–472.
- [9] A. El Nemr, M.M. El-Sadaawy, A. Khaled, S.O. Draz, Aliphatic and polycyclic aromatic hydrocarbons in the surface sediments of the Mediterranean: Assessment and source recognition of petroleum hydrocarbons, *Environ. Monit. Assess.* 185(6) (2013) 4571–4589.
- [10] B.R.T. Simoneit, Biomass burning—A review of organic tracers for smoke from incomplete combustion, *Appl. Geochem.* 17 (2002) 129–162.
- [11] R.M. Dickhut, R.E. Countway, E.A. Canuel, Polycyclic aromatic hydrocarbon (PAH) distributions and association with organic matter in surface waters of the York River, VA estuary, *Org. Geochem.* 34 (2003) 209–224.
- [12] A. El Nemr, Petroleum contamination in warm and cold marine environment, Nova Science, Hauppauge, NY, 2005.
- [13] A. El Nemr, Impact, monitoring and management of environmental pollution, Nova Science, Hauppauge, NY, 2010.
- [14] A. El Nemr, A. Khaled, A. El-Sikaily, T.O. Said, A.M.A. Abd-Allah, Distribution and sources of polycyclic aromatic hydrocarbons in surface sediments of the Suez Gulf, *Environ. Monit. Assess.* (2006), doi: 10.1007/s10661-005-9009-4.
- [15] I.A. Ololade, Prediction of polycyclic aromatic hydrocarbons toxicity using equilibrium partitioning approach and Narcosis model, *Bull. Environ. Contam. Toxicol.* 85 (2010) 238–242.
- [16] L.P. da Luz, P.J.S. Filho, E.E.H. de Sousa, T. Kerstner, E.B. Caramão, Evaluation of surface sediment contamination by polycyclic aromatic hydrocarbons in colony Z3—(Patós Lagoon, Brazil), *Microchem. J.* 96 (2010) 161–166.
- [17] C.W. Chen, C.F. Chen, Distribution, origin, and potential toxicological significance of polycyclic aromatic hydrocarbons (PAHs) in sediments of Kaohsiung Harbor, Taiwan. *Mar. Pollut. Bull.* 63 (2011) 417–423.
- [18] N. Bihari, M. Fafandel, B. Hamer, B. Kralj-Bilen, PAH content, toxicity and genotoxicity of coastal marine sediments from the Rovinj area, Northern Adriatic, Croatia, *Sci. Total Environ.* 366(2–3) (2006) 602–611.
- [19] H. Budzinski, I. Jones, J. Bellocq, C. Pierard, P. Garrigues, Evaluation of sediment contamination by polycyclic aromatic hydrocarbons in the Gironde estuary, *Mar. Chem.* 58 (1997) 85–97.
- [20] P. Baumard, H. Budzinski, P. Garrigues, Polycyclic aromatic hydrocarbons in sediments and mussels of the western Mediterranean Sea, *Environ. Toxicol. Chem.* 17 (1998) 765–776.
- [21] J.W. Readman, G. Fillmann, I. Tolosa, J. Bartocci, J.P. Villeneuve, C. Catinni, L.D. Mee, Petroleum and PAH contamination of the Black Sea, *Mar. Pollut. Bull.* 44 (2002) 48–62.
- [22] K. Maskaoui, H. Zhong, Contamination and ecotoxicology risks of polycyclic aromatic hydrocarbons in Shantou coastal waters, China. *Bull. Environ. Contam. Toxicol.* 82 (2009) 172–178.
- [23] G.P. Yang, Polycyclic aromatic hydrocarbons in sediments of the South China Sea, *Environ. Pollut.* 108 (2000) 163–171.
- [24] UNEP/IOC/IAEA, Sampling of Selected Marine Organisms and Sample Preparation for The Analysis Of Chlorinated Hydrocarbons, Reference Methods for Marine Pollution Studies no. 12, Revision 2, United Nations Environment Programme 17, Nairobi, 1991.

- [25] UNEP/IOC/IAEA, Determination of petroleum hydrocarbons in sediments, reference methods for marine pollution studies, UNEP, 20 (1992) 75 pp.
- [26] R.L. Folk, Petrology of sedimentary rocks, Hemphill Publication Cooperation, Austin, TX, 1954.
- [27] J.S. Galehouse, Sedimentation analysis, In: R.E. Carver (Ed), Procedures in sedimentary petrology, Wiley, New York, NY, pp. 69–94, 1971.
- [28] M. Ehrhardt, Liophilic organic material: An apparatus for extracting solids used for their concentration from seawater, ICES Techn. Environ. Sci. 4 (1987) 1–14.
- [29] D.H. Loring, R.T.T. Rantala, Manual for the geochemical analysis of marine sediment and suspended particulate matter, Earth-Sci. Rev. 32 (1992) 255–285.
- [30] B.F. Molnia, A rapid and accurate method for the analysis of calcium carbonate in small samples, J. Sed. Petrol. 44(2) (1974) 589–590.
- [31] USEPA (U.S. Environmental Protection Agency), Human Health Evaluation Manual, Supplemental Guidance: "Standard Default Exposure Factors", OSWER Directive 9285.6-03, 1991.
- [32] USEPA (U.S. Environmental Protection Agency), Risk Assessment Guidance for Superfund, Volume I Human Health Evaluation Manual (Part A), EPA/540/1, 1989.
- [33] C.D. Simpson, A.A. Mosi, W.R. Cullen, K.J. Reimer, Composition and distribution of polycyclic aromatic hydrocarbon contamination in surficial marine sediment from Kitimat harbor Canada, Sci. Total. Environ. 181 (1998) 265–278.
- [34] A. El Nemr, Organic hydrocarbons in surface sediments of the Mediterranean coast of Egypt: Distribution and sources, Egypt. J. Aquat. Res. 34(3) (2008) 36–57.
- [35] S.de Mora, I. Tolosa, S.W. Fowler, J.P. Villeneuve, R. Cassi, C.Cattini, Distribution of petroleum hydrocarbons and organochlorinated contaminants in marine biota and coastal sediments from the ROPME Sea Area during 2005, Mar. Pollut. Bull. 60(12) (2010) 2323–2349.
- [36] O.E. Oyo-Ita, B.O. Ekpo, D.R. Orosa, Distributions and sources of aliphatic hydrocarbons and ketones in surface sediments from the Cross River estuary, S.E. Niger Delta, Nigeria, J. Appl. Sci. Environ. Sanita. 5(1) (2010) 1–11.
- [37] F.G. Prahl, J.R. Ertel, M.A. Goni, M.A. Sparrow, B. Eversmeyer, Terrestrial organic carbon contributions to sediments on the Washington margin, Geochim. Cosmochim. Ac. 58 (1994) 3035–3048.
- [38] X.C. Wang, S. Sun, H.Q. Ma, Y. Liu, Sources and distribution of aliphatic and polyaromatic hydrocarbons in sediments of Jiaozhou Bay, Qingdao, China, Mar. Pollut. Bull. 52 (2006) 129–138.
- [39] P. Gearing, J. Gearing, T.F. Lytle, J. Lytle, Hydrocarbons in 60 northeast Gulf of Mexico shelf sediments: A preliminary survey, Geochim. Cosmochim. Ac. 40 (1976) 1005–1017.
- [40] M.G. Commendatore, J.I. Esteves, J.C. Colombos, Hydrocarbons in coastal Sediments of Patagonia, Argentina: Levels and probable sources, Mar. Pollut. Bull. 40 (2000) 989–998.
- [41] J. Allan, A.G. Douglas, Variations in the content and distribution of n-alkanes in a series of Carboniferous vitrinites and sporinites of bituminous rank, Geochim. Cosmochim. Ac. 41 (1977) 1223–1230.
- [42] A. Pearson, T.I. Eglinton, The origin of n-alkanes in Santa Monica Basin surface sediment: A model based on compound-specific  $^{14}\text{C}$  and  $^{13}\text{C}$  data, Org. Geochem. 31 (2000) 1103–1116.
- [43] X.C. Wang, R.F. Chen, A. Berry, Sources and preservation of organic matter in Plum Island salt marsh sediments (MA, USA): Longchain n-alkanes and stable carbon isotope compositions. Estuarine, Coast. She. Sci. 58 (2003) 917–928.
- [44] R.A. Bourbonniere, P.A. Meyers, Sedimentary geolipid records of historical changes in the watersheds and productivities of Lakes Ontario and Erie, Limnol. Oceanogr. 41 (1996) 352–359.
- [45] C.R. de Oliveira, L.A.d.S. Madureira, Assessment and sources of nonaromatic hydrocarbons in surface sediments of three harbors in Santa Catarina State, Brazil, Environ. Monit. Assess. 173 (2011) 91–105.
- [46] K.J. Ficken, B. Li, D.L. Swain, G. Eglinton, An n-alkane proxy for the sedimentary input of submerged/floating freshwater aquatic macrophytes, Org. Geochem. 31 (2000) 745–749.
- [47] R. Mead, Y. Xu, J. Chong, R. Jaffe, Sediment and soil organic matter source assessment as revealed by the molecular distribution and carbon isotopic composition of n-alkanes, Org. Geochem. 36 (2005) 363–370.
- [48] F. Beolchini, L. Rocchetti, F. Regoli, A. Dell'Anno, Bioremediation of marine sediments contaminated by hydrocarbons: Experimental analysis and kinetic modeling, J. Hazard. Mater. 182 (2010) 403–407.
- [49] G. Witt, Polycyclic aromatic hydrocarbons in water and sediment of the Baltic Sea, Mar. Pollut. Bull. 31 (1995) 237–248.
- [50] L. Viñas, M.A. Franco, J.A. Soriano, J.J. González, J. Pon, J. Albaigés, Sources and distribution of polycyclic aromatic hydrocarbons in sediments from the Spanish northern continental shelf. Assessment of spatial and temporal trends, Environ. Pollut. 158 (2010) 1551–1560.
- [51] S.G. Wakeham, Aliphatic and polycyclic hydrocarbons in Black Sea sediments, Mar. Chem. 53 (1996) 187–205.
- [52] A.R. Mostafa, T.L. Wade, S.T. Sweet, A.K.A. Al-Alimi, Distribution and characteristics of polycyclic aromatic hydrocarbons (PAHs) in sediments of Hadhramout coastal area, Gulf of Aden, Yemen, J. Mar. Syst. 78 (2009) 1–8.
- [53] E. Lipiatou, A. Saliot, Fluxes and transport of anthropogenic and natural polycyclic aromatic hydrocarbons in the western Mediterranean Sea, Mar. Chem. 32 (1991) 51–71.
- [54] P. Baumard, H. Budzinski, P. Garrigues, H. Dizer, P.D. Hansen, Polycyclic aromatic hydrocarbons in recent sediments and mussels (*Mytilus edulis*) from the Western Baltic Sea: Occurrence, bioavailability and seasonal variations, Mar. Environ. Res. 47 (1999) 17–47.
- [55] A. Gogou, I. Bouloubassi, E.G. Stephanou, Marine organic geochemistry of the Eastern Mediterranean: 1. Aliphatic and polyaromatic hydrocarbons in Cretan Sea surficial sediments, Mar. Chem. 68 (2000) 265–282.
- [56] L. Tolun, D. Martens, O.S. Okay, K.W. Schramm, Polycyclic aromatic hydrocarbon contamination in coastal sediments of the Izmit Bay (Marmara Sea): Case studies before and after the Izmit earthquake, Environ. Int. 32 (2006) 758–765.
- [57] S. Ünlü, B. Alpar, Distribution and sources of hydrocarbons in surface sediments of Gemlik Bay (Marmara Sea, Turkey), Chemosphere 64 (2006) 764–777.
- [58] A. El Nemr, T.O. Said, A. Khaled, A. El-Sikaily, A.M.A. Abd-Allah, The distribution and sources of polycyclic aromatic hydrocarbons in surface sediments along the Egyptian Mediterranean coast, Environ. Monit. Assess. 124 (2007) 343–359.
- [59] B. Karacik, O.S. Okay, B. Henkelmann, S. Bernhöft, K.W. Schramm, Polycyclic aromatic hydrocarbons and effects on marine organisms in the Istanbul Strait, Environ. Int. 35 (2009) 599–606.
- [60] IARC (International Agency for Research on Cancer), IARC Monographs on the Evaluation of the Carcinogenic Risk of Chemicals to Human, Polynuclear Aromatic Compounds, Part I, Chemical, Environmental, and Experimental Data, World Health Organization, Geneva, 1983.
- [61] C.A. Menzie, B.B. Potocki, J. Santodonato, Exposure to carcinogenic PAHs in the environment, Environ. Sci. Technol. 26 (1992) 1278–1284.
- [62] C.Y. Kuo, Y.W. Cheng, Y.W. Chen, H. Lee, Correlation between the amounts of polycyclic aromatic hydrocarbons and mutagenicity of airborne particulate samples from Taichung City, Taiwan, Environ. Res. Sec. A. 78 (1998) 43–49.

- [63] X.L. Wang, S. Tao, R.W. Dawson, F.L. Xu, Characterizing and comparing risks of polycyclic aromatic hydrocarbons in a Tianjin wastewater-irrigated area, *Environ. Res.* 90 (2002) 201–206.
- [64] K. Srogi, Monitoring of environmental exposure to polycyclic aromatic hydrocarbons: A review, *Environ. Chem. Lett.* 5 (2007) 169–195.
- [65] E.R. Long, L.J. Field, D.D. MacDonald, Predicting toxicity in marine sediments with numeral sediment quality guidelines, *Environ. Toxicol. Chem.* 17 (1998) 714–727.
- [66] E.R. Long, D.D. MacDonald, Incidence of adverse biological effects within ranges of chemical concentration in marine and estuarine sediments, *Environ. Manage.* 19 (1995) 81–97.
- [67] CCME (Canadian Council of Ministers of the Environment), Canadian Sediment Quality Guidelines for the Protection of Aquatic Life, Canadian Environmental Quality Guidelines Canadian Council of Ministers of the Environment, Winnipeg, 2002.
- [68] CCME (Canadian Council of Ministers of the Environment), Canadian sediment quality guidelines for the protection of aquatic life, 2001. Available from: <http://www.ec.gc.ca/ceqrcq/sediment.htm>
- [69] L.T. Gonul, F. Kucuksezgin, Aliphatic and polycyclic aromatic hydrocarbons in the surface sediments from the Eastern Aegean: Assessment and source recognition of petroleum hydrocarbons, *Environ. Sci. Pollut. Res.* 19(1) (2012) 31–41.
- [70] C.L. Gigliotti, P.A. Brunciak, J. Dachs, T.R. IV Glenn, E.D. Nelson, L.A. Totten, S.J. Eisenreich, Air–water exchange of polycyclic aromatic hydrocarbons in the New York–New Jersey, USA, harbor estuary, *Environ. Toxicol. Chem.* 21(2) (2002) 235–244.
- [71] J. Tolosa, J.M. Bayona, J. Albaige's, Aliphatic and polycyclic aromatic hydrocarbons and sulfur/oxygen derivatives in northwestern Mediterranean sediments: Spatial and temporal variability, fluxes, and budgets, *Environ. Sci. Technol.* 30 (1996) 2495–2503.
- [72] J.L. Lake, C. Norwood, C. Dimock, R. Bowen, Origins of polycyclic aromatic hydrocarbons in estuarine sediments, *Geochim. Cosmochim. Ac.* 43 (1979) 1847–1854.
- [73] R.E. Laflamme, R.A. Hites, The global distribution of PAH in recent sediments, *Geochim. Cosmochim. Ac.* 42 (1978) 289–303.
- [74] M.L. Lee, G.P. Prado, J.B. Howard, R.A. Hites, Source identification of urban airborne polycyclic aromatic hydrocarbons by gas chromatography—Mass spectrometry and high resolution mass spectrometry, *Biomed. Mass. Spectrom.* 4(3) (1977) 182–186.
- [75] A. Malik, P. Verma, A.K. Singh, K.P. Singh, Distribution of polycyclic aromatic hydrocarbons in water and bed sediments of the Gomti River, India, *Environ. Monit. Assess.* 172 (2011) 529–545.
- [76] A. Hites, R.E. LaFlamme, J.G. Windsor, Polycyclic aromatic hydrocarbons in marine/aquatic sediments: Their ubiquity, In: L. Oettrakis, F. Weiss (Eds), *Petroleum in the Marine Environment*, Advance in Chemistry Series, vol. 185, ACS, Washington, DC, pp. 289–311, 1980.
- [77] G. De Luca, A. Futionio, R. Leardo, G. Micera, A. Panzanelli, P.C. Piu, G. Sanna, Polycyclic aromatic hydrocarbons assessment in the sediments of the Porto Torre Harbor (Northern Sardinia, Italy), *Mar. Chem.* 86 (2004) 15–32.
- [78] H.H. Soclo, P. Garrigues, M. Ewald, Origin of polycyclic aromatic hydrocarbons (PAHs) in coastal marine sediments: Case studies in Cotonou (Benin) and Aquitaine (France) areas, *Mar. Pollut. Bull.* 40 (2000) 387–396.
- [79] H.M. Hwang, T.L. Wade, J.L. Sericano, Concentrations and source characterization of polycyclic aromatic hydrocarbons in pine needles from Korea, Mexico, and United States, *Atmosph. Environ.* 37 (2003) 2259–2267.
- [80] M.B. Yunker, R.W. Macdonald, R. Vingarzan, R.H. Mitchell, D. Goyette, S. Sylvestre, PAHs in the Fraser river basin: A critical appraisal of PAH ratios as indicators of PAH source and composition, *Org. Geochem.* 33 (2002) 489–515.
- [81] ANZECC & ARMCANZ, Australian and New Zealand Guidelines for Fresh and Marine Water Quality. Volume 1, Section 3.5: Sediment Quality Guidelines, Australian and New Zealand Environment and Conservation Council, and Agriculture and Resource Management Council of Australia and New Zealand, Canberra, 2000.